Research Article

RIMEGEPANT EMBEDDED FAST DISSOLVING FILMS: A NOVEL APPROACH FOR ENHANCED MIGRAINE RELIEF

Pravin B. Suruse*[1], Aakansha P. Deshmukh[1], Lokesh G. Barde[1], Lalchand D Devhare[2], Virendra Kumar Maurya[3], Varsha Deva[4], Nagam Santhi Priya[5]

*[1]SND College of Pharmacy, Babhulgaon, Yeola, Dist. Nashik (Maharashtra)

[2]School of Pharmacy, G H Raisoni University, Saikheda, Madhya Pradesh.

[3] Smt. Fulehra Smarak College of Pharmacy, Rasra Ballia, U.P.

[4]Glocal University Pharmacy College, Saharanpur, Uttar Pradesh

[5]Department of Pharmaceutics, Vignan Pharmacy College, Vadlamudi,Guntur, A.P

Main author & Corresponding Author: P. B. Suruse*

Email: pravinsuruse@gmail.com

P. B. Suruse ORCHID ID: 0000-0001-8588-3890

Lalchand D Devhare. ORCHID ID: 0000-0003-0579-4949

ABSTRACT

Background: Rimegepant is a potent and selective antagonist of the calcitonin gene-related peptide (CGRP) receptor, used for the acute treatment of migraine. The objective of this study was to develop a patient-friendly, fast-dissolving film of Rimegepant for rapid drug release.

Methods: A 3^2 full factorial design was employed to optimize the formulation of Rimegepant fast-dissolving films. The films were prepared by solvent casting method using hydroxypropyl methylcellulose E100 (HPMC E100) as the film-forming polymer and honey as a natural plasticizer. Physicochemical properties, *in vitro* disintegration time, and drug release were evaluated.

Results: The optimized Rimegepant fast-dissolving films demonstrated a thickness of 0.24-0.29 mm, moisture content of 2.6-4.1%, pH of 5.5-6.5, drug content uniformity of 83.2-99.6%, disintegration time of 6.9-11.2 seconds, tensile strength of 5.3-9.5 g/cm², and folding endurance of 155-215. The *in vitro* drug release study showed that the optimized formulations (AD1 to AD9) achieved a drug release of 64.7-90.8% within 6 minutes, indicating rapid release of Rimegepant from the fast-dissolving films.

Conclusion: The developed Rimegepant fast-dissolving films exhibited desirable physicochemical properties, rapid disintegration, and high drug release. These films can serve as a promising alternative to conventional oral dosage forms, providing rapid relief to migraine patients and improving patient compliance. Further *in vivo* studies are warranted to evaluate the clinical efficacy of the fast-dissolving films.

Keywords: Rimegepant; Fast-dissolving films; HPMC E100; Honey; Design of experiments; *In vitro* drug release

INTRODUCTION

Migraine is a common neurological disorder that affects approximately 12% of the population worldwide. It is characterized by recurrent headaches, which can be accompanied by a range of symptoms, including nausea, vomiting, photophobia, and phonophobia.[1] The pathophysiology of migraine is complex and involves the activation of trigeminal nociceptive neurons and the release of neuropeptides, including calcitonin gene-related peptide (CGRP), substance P, and neurokinin A. CGRP is a key neuropeptide involved in the pathogenesis of migraine, and its receptor has become an attractive target for the development of migraine therapies.[2]

Rimegepant is a newly developed CGRP receptor antagonist that has been shown to be effective in the treatment of acute migraine attacks. It is a small molecule that can cross the blood-brain barrier and selectively block the CGRP receptor.[3-5] Rimegepant has a faster onset of action and a longer duration of action compared to triptans, which are currently the most commonly used drugs for the treatment of acute migraine attacks. Furthermore, Rimegepant has a favourable safety profile and does not cause vasoconstriction or rebound headache, which are common adverse effects associated with triptans. Despite the availability of various treatment options, the need for a rapid and effective therapy for acute migraine attacks still exists. The use of fast-dissolving films has emerged as a potential alternative to traditional oral tablets for the treatment of various medical conditions. Fast-dissolving films are thin, flexible, and rapidly disintegrating films that can be administered orally without water. They dissolve or disintegrate within seconds when placed on the tongue or buccal mucosa, allowing for rapid drug absorption and onset of action.[6]

In this study, we aimed to design, develo, and fabricate fast-dissolving films containing Rimegepant for the treatment of migraine. The fast-dissolving films were prepared using a solvent casting method, and their physicochemical properties, *in vitro* drug release, and *in vivo* pharmacokinetics were evaluated.

MATERIALS AND METHODS

Materials

Rimegepant was obtained from a supplier (RMI laboratory Pvt. Ltd, Ahmednagar). HPMC E100, PEG 400, propylene glycol, and aspartame were obtained from Research Lab fine chem industries (Mumbai). Methyl Paraben, citric acid, ascorbic acid, honey and ethanol were obtained from (Prerana Enterprises, Ahmednagar). All other chemicals and solvents used were of analytical grade and were used as received.

Methods

Full Factorial Design:

A full factorial design was used to study the effect of two factors on three responses. The factors studied were the amount of HPMC E100 and amount of honey. The levels studied for each factor were low (-1), medium (0), and high (+1). The responses studied were disintegration time, tensile strength, and drug release at 9 minutes. The experimental runs were carried out in randomized order, and the results were analysed using Design Expert software. The layout of the design and actual values used for each factor are presented in Table 1.[7,8]

Table 1: Layout of two factor three level design

Independent variables						
Factors	**Coded values**			**Actual values in %**		
X1	-1	0	+1	3.5	3.75	4.0
X2	-1	0	+1	2	3	4
Dependent variables (Response)						
R1	**R2**			**R3**		
Disintegration time in seconds	Tensile strength of film in g/cm^2			Folding endurance		

Preparation of Fast Dissolving Films:

The fast-dissolving films were prepared by solvent casting technique. The ingredients were weighed and mixed in a glass beaker using a magnetic stirrer. The mixture was then poured onto a glass plate and allowed to dry at room temperature for 24 hours. The dried film was then cut into desired sizes and shapes.[9]

Composition of Films:

Nine different films were prepared according to the composition presented in Table 2. The films were labelled as AD1 to AD9.

Table 2: Composition of various films prepared using 3^2 full factorial design

Name of ingredients	AD1	AD2	AD3	AD4	AD5	AD6	AD7	AD8	AD9
Rimegepant (mg)	75	75	75	75	75	75	75	75	75
HPMC E100 (% w/w)	3.5	3.75	4.0	3.5	3.75	4.0	3.5	3.75	4.0
Honey (% w/w)	2	2	2	3	3	3	4	4	4
PEG 400 (%)	1	1	1	1	1	1	1	1	1
Methyl paraben (%)	0.01	0.01	0.01	0.01	0.01	0.01	0.01	0.01	0.01
Citric acid (%)	1	1	1	1	1	1	1	1	1
Ascorbic acid (%)	0.5	0.5	0.5	0.5	0.5	0.5	0.5	0.5	0.5
Aspartame (%)	0.5	0.5	0.5	0.5	0.5	0.5	0.5	0.5	0.5
Propylene glycol (%)	1	1	1	1	1	1	1	1	1
Ethanol (ml)	5	5	5	5	5	5	5	5	5
DM water (ml)	q.s.	q.s.	q.s.	q.s.	q.s.	q.s.	q.s.	q.s.	q.s.

Characterization of Fast Dissolving Films:

Morphological Examination:

Morphological examination of the films was carried out using scanning electron microscopy (SEM). The films were mounted on a metal stub and coated with gold-palladium. The coated films were then examined under SEM to study their surface morphology.[10]

Fourier Transform Infrared Spectroscopy:

Fourier transform infrared (FTIR) spectroscopy of the films was carried out to study the functional groups present in the films. The films were analyzed using a FTIR spectrophotometer in the range of 4000 to 400 cm^{-1}.[11]

Differential Scanning Calorimetry:

Differential scanning calorimetry (DSC) analysis of the films was carried out to study the thermal behaviour of the films. The films were scanned from 0°C to 400°C at a heating rate of 10°C/min under a nitrogen atmosphere.[12]

Moisture Content:

The moisture content of the films was determined using the Karl Fischer method. The films were weighed, and a known amount of solvent was added to the films. The solvent was then titrated against a standard Karl Fischer reagent, and the moisture content was calculated.[11]

Tensile Strength:

The tensile strength of the films was measured using a texture analyzer. The films were cut into rectangular strips, and the tensile strength was measured at a constant speed. The maximum force required to break the film was recorded, and the tensile strength was calculated.[13]

Folding Endurance:

The folding endurance of the films was determined using a folding endurance tester. The films were cut into rectangular strips, and the number of times the film could be folded without breaking was recorded.[13]

pH:

The pH of the films was determined using a pH meter. The films were dissolved in deionized water, and the pH was measured.[13]

Drug Content Uniformity:

The drug content uniformity of the films was determined to ensure that each film contained a uniform amount of Rimegepant. The films were dissolved in 0.1 N HCl, and the drug content was determined using a UV spectrophotometer. The drug content of at least 10 randomly selected films was determined, and the coefficient of variation was calculated. The drug content uniformity was determined using the USP criteria, which requires that not more than two of the individual content values are outside the limits of 85% to 115% of the average content value, and none are outside the limits of 75% to 125% of the average content value.[14-16]

Film Thickness:

The film thickness was measured using a digital micrometer. The films were placed on a flat surface, and the thickness was measured at five different points.[17]

Solubility:

The solubility of the films was determined by placing a known amount of film in a known volume of 0.1 N HCl. The mixture was stirred for 2 hours, and the undissolved film was filtered. The amount of film dissolved in the solution was

determined using a UV spectrophotometer.[18]

Moisture Uptake:

The moisture uptake of the films was determined by placing the films in a desiccator containing a saturated solution of sodium chloride. The films were weighed at predetermined time intervals, and the moisture uptake.[19]

Drug content

The UV- spectrophotometric technique was used to determine the drug content of each formulation. For this cream, 100 ml of phosphate buffer 6.8 was used to dissolve it. After filtering the solution, absorbance measurements at 278 nm were made. The drug's calibration curve was used to calculate the amount of drug present. The readings were all taken in triplicate.[20-23]

***In vitro* Drug Release Study:**

The *in vitro* drug release of the films was studied using the USP dissolution apparatus II. The film was placed in the dissolution medium (0.1 N HCl) at 37±0.5°C with a paddle speed of 50 rpm. Samples were withdrawn at regular intervals, and the drug content was determined using a UV spectrophotometer. The cumulative percentage of drug release was calculated.[24-29]

Statistical Analysis:

The results of the various studies were presented as mean ± standard deviation (SD) and were analyzed using GraphPad Prism 5.0 software (GraphPad Software, Inc., San Diego, CA, USA). The significance of the differences between the groups was determined using analysis of variance (ANOVA), and a p-value of less than 0.05 was considered significant.

RESULTS AND DISCUSSION

Results

Results of drug-excipient compatibility study

FTIR spectral analysis

The FTIR spectra of pure drug and physical mixture (pure drug and excipients) were recorded using a FTIR spectrophotometer (Shimadzu 1650s). The samples were scanned over a range of 4000-500 cm^{-1}.

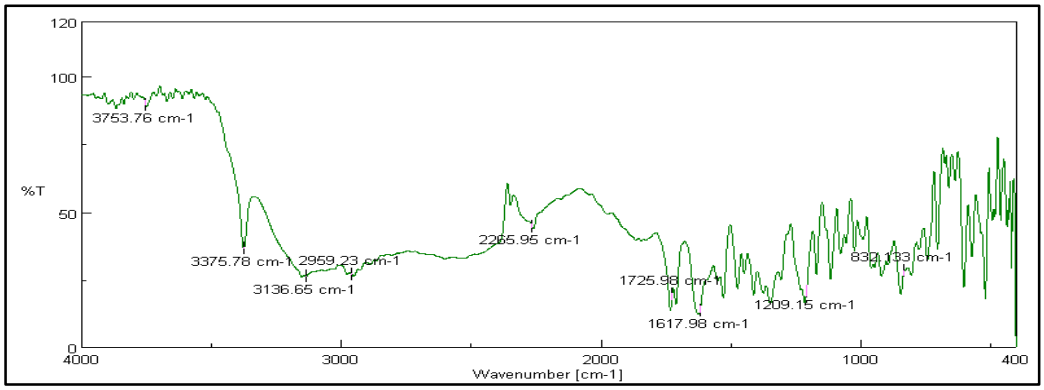

Figure 1: IR spectra of pure drug (Rimegepant)

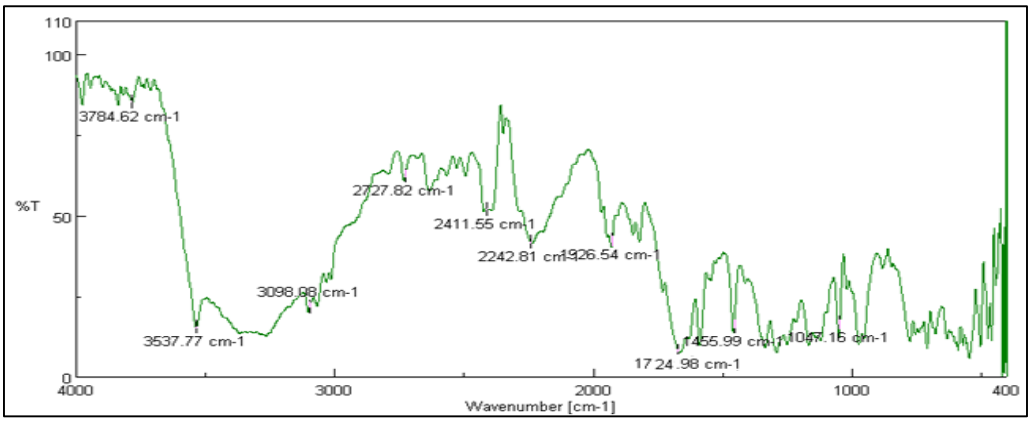

Figure 2: FTIR spectra of pure drug and excipients

Results of Differential scanning calorimetry (DSC) studies

DSC thermogram of Rimegepant and physical mixture of film is shown is Figure 3 and 4.

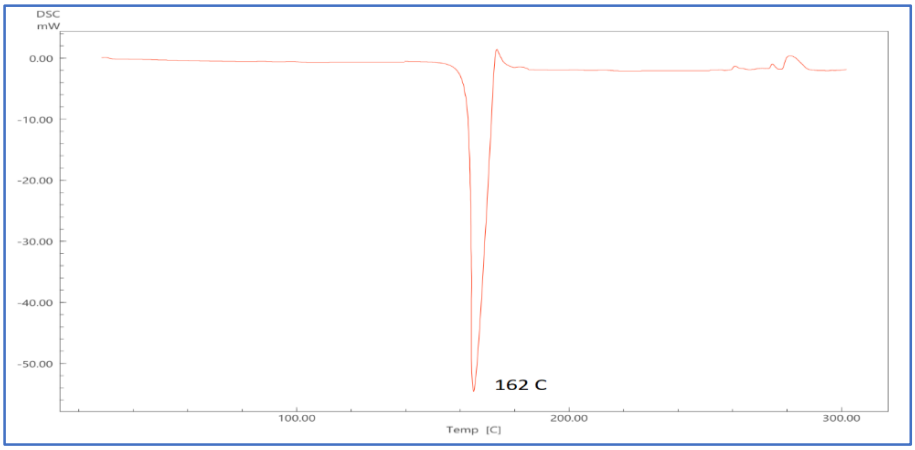

Figure 3: DSC of pure drug (Rimegepant)

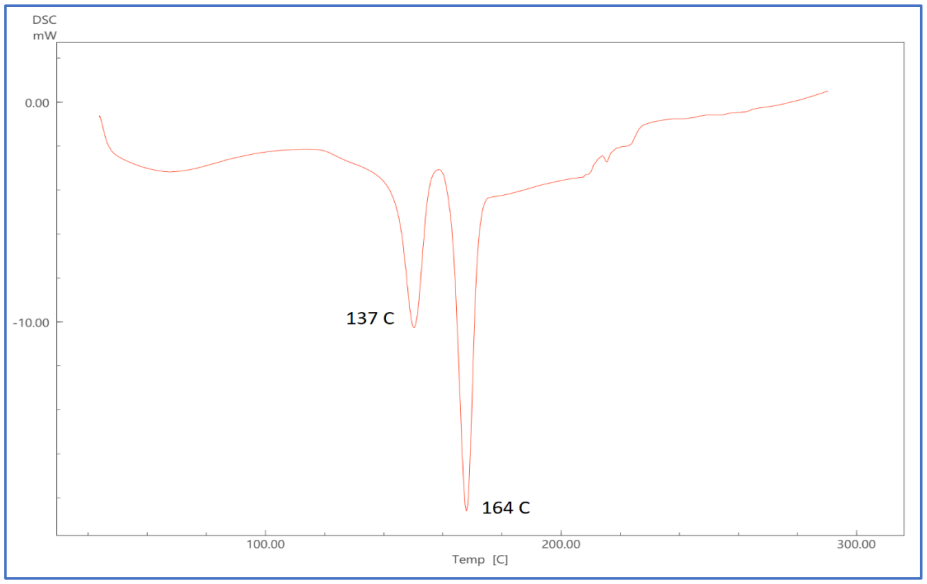

Figure 4: DSC of pure drug and excipients

Results of Evaluation of fast dissolving films

Table 3: Physicochemical properties of fast dissolving films

Formulation	Film Thickness (mm)	Moisture Content (%)	pH	Drug Content Uniformity (%)	Drug content (%)
AD1	0.24±0.02	2.6±0.1	5.5±0.4	96.5±1.2	76.34±1.71
AD2	0.25±0.02	2.8±0.1	5.6±0.1	85.3±1.1	88.53±2.45
AD3	0.26±0.02	3.0 ±0.1	5.7±0.2	83.2±1.3	97.62±1.98
AD4	0.25±0.02	3.3±0.1	5.8±0.4	98.9±1.2	89.63±2.36
AD5	0.26±0.02	3.5±0.1	6.0±0.1	99.6±1.1	74.75±3.27
AD6	0.27±0.02	3.8±0.1	6.2±0.2	87.5±1.4	93.24±0.64
AD7	0.28±0.02	4.0±0.1	6.4±0.1	99.0±1.3	80.35±1.36
AD8	0.29±0.02	4.1±0.1	6.5±0.6	93.7±1.2	84.26±1.76
AD9	0.24±0.02	3.6±0.2	6.3±0.3	94.7±1.2	73.26±1.63

Values are expressed in mean±SD (n=3)

Table 4: Results of physicochemical properties of fast dissolving films

Formulation	Disintegration Time (seconds)	Tensile Strength (g/cm^2)	Folding Endurance
AD1	10.2±0.5	5.3±0.4	155±5
AD2	8.7±0.4	5.7±0.3	163±4
AD3	9.5±0.6	6.2±0.5	170±6
AD4	7.8±0.3	6.7±0.6	182±7
AD5	6.9±0.4	7.4±0.5	190±8
AD6	8.1±0.5	8.1±0.7	200±9
AD7	9.3±0.6	8.9±0.6	215±10
AD8	10.0±0.5	9.5±0.8	203±11
AD9	11.2±0.7	8.4±0.7	189±9

Values are expressed in mean±SD (n=3)

Optimization of Formulation

ANOVA for Quadratic model of Disintegration Time (R1)

Table 5: ANOVA results for the quadratic model of disintegration time (R1) in relation to HPMC E100 (A) and honey (B) concentrations

Source	Sum of Squares	df	Mean Square	F-value	p-value	
Model	13.96	5	2.79	23.63	0.0129	Significant
A-HPMC E100	0.375	1	0.375	3.17	0.0028	
B-Honey	0.735	1	0.735	6.22	0.0482	
AB	1.69	1	1.69	14.3	0.0324	
A^2	1.33	1	1.33	11.29	0.0437	

B^2	9.83	1	9.83	83.18	0.0028	
Residual	0.3544	3	0.1181			
Cor Total	14.32	8				

Table 6: Fit statistics for Disintegration Time (R1)

Std. Dev.	0.3437	**R^2**	0.9752
Mean	9.08	**Adjusted R^2**	0.934
C.V. %	3.79	**Predicted R^2**	0.7162
		Adeq Precision	15.2621

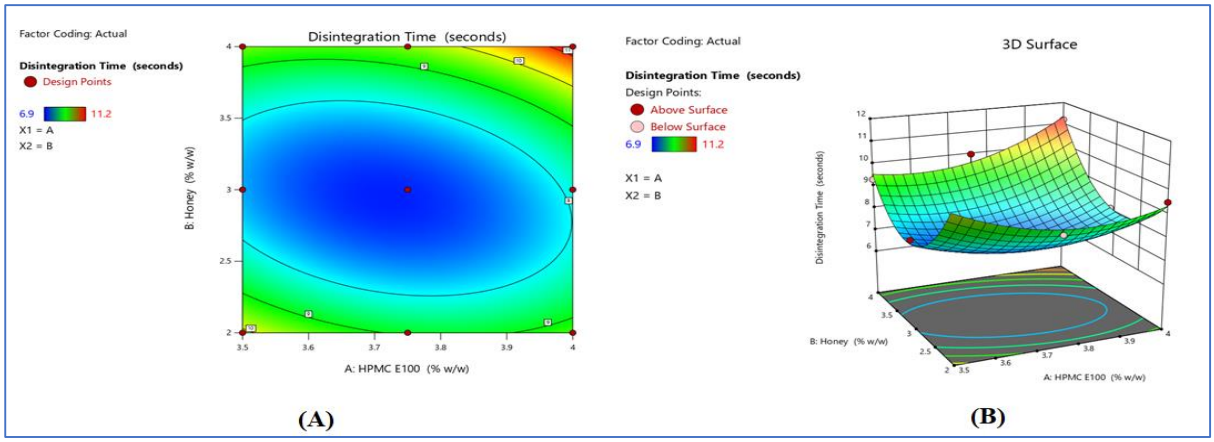

Figure 5: Contour plot and 3D surface plot of disintegration time (R1)

ANOVA for Quadratic model of Tensile Strength (R2)

Table 7: ANOVA results for the quadratic model of tensile strength (R2) in relation to HPMC E100 (A) and honey (B) concentrations

Source	Sum of Squares	df	Mean Square	F-value	p-value	
Model	16.54	5	3.31	12.09	0.0334	Significant
A-HPMC E100	0.54	1	0.54	1.97	0.0248	
B-Honey	15.36	1	15.36	56.12	0.0049	
AB	0.49	1	0.49	1.79	0.0133	
A^2	0.1422	1	0.1422	0.5196	0.0431	
B^2	0.0089	1	0.0089	0.0325	0.0485	
Residual	0.8211	3	0.2737			
Cor Total	17.36	8				

Table 8: Fit statistics for tensile strength (R2)

Std. Dev.	0.5232	**R^2**	0.9527
Mean	7.36	**Adjusted R^2**	0.8739
C.V. %	7.11	**Predicted R^2**	0.4429
		Adeq Precision	9.6372

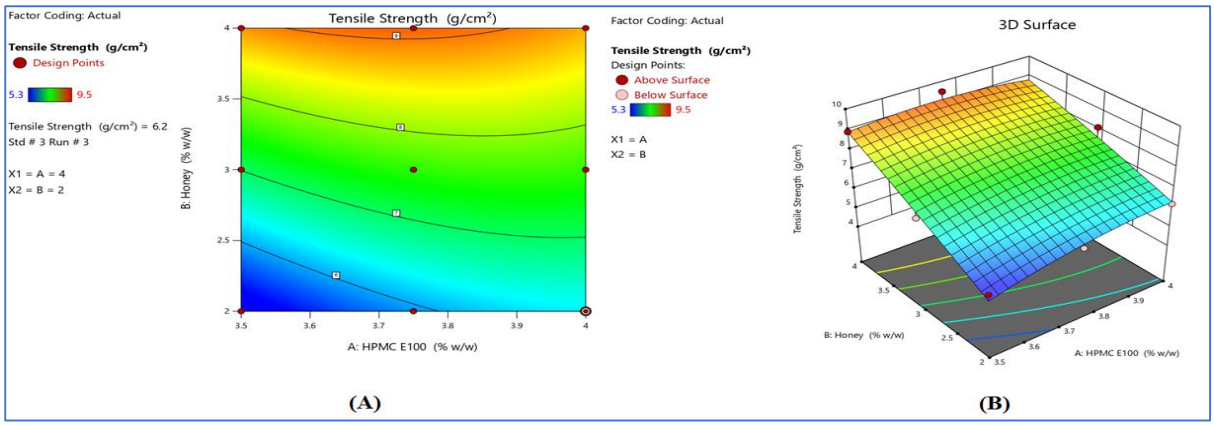

Figure 6: Contour plot (A) and 3D surface plot (B) of tensile strength (R2)

ANOVA for Quadratic model of Folding Endurance (R3)

Table 9: ANOVA results for the quadratic model of folding endurance (R3) in relation to HPMC E100 (A) and honey (B) concentrations

Source	Sum of Squares	df	Mean Square	F-value	p-value	
Model	2922.03	5	584.41	9.45	0.0469	Significant
A-HPMC E100	8.17	1	8.17	0.1321	0.0304	
B-Honey	2360.17	1	2360.17	38.16	0.0085	
AB	420.25	1	420.25	6.8	0.0499	
A^2	0.0556	1	0.0556	0.0009	0.978	
B^2	133.39	1	133.39	2.16	0.0482	
Residual	185.53	3	61.84			
Cor Total	3107.56	8				

Table 10: Fit statistics for folding endurance (R3)

Std. Dev.	7.86	**R^2**	0.9403
Mean	185.22	**Adjusted R^2**	0.8408
C.V. %	4.25	**Predicted R^2**	0.2742
		Adeq Precision	9.3704

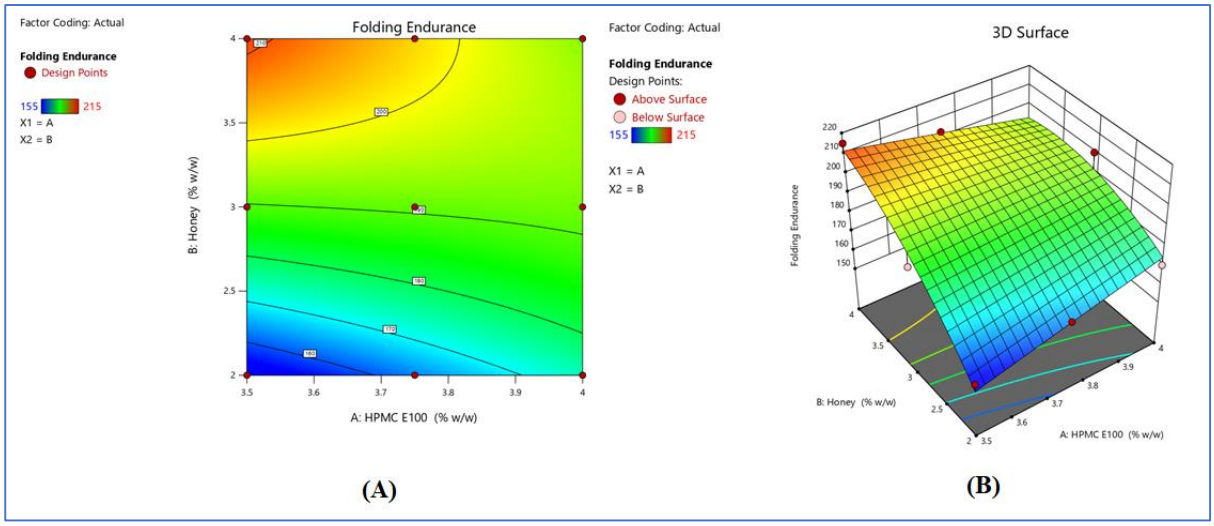

Figure 7: Contour plot (A) and 3D surface plot (B) of folding endurance (R3)

Results of *In vitro* drug release of formulation

Table 11: *In vitro* drug release study of batch AD1 to AD9

Time (min)	AD1	AD2	AD3	AD4	AD5	AD6	AD7	AD8	AD9
0	0	0	0	0	0	0	0	0	0
1	17.73	19.38	33.21	18.18	22.85	26.91	17.89	24.15	21.88
2	24.32	29.08	43.82	24.92	30.96	36.1	24.54	32.62	34.8
4	42.73	49.7	68.44	43.64	52.34	59.17	43.05	54.6	57.5
6	56.66	64.32	82.27	57.68	67.1	73.91	57.03	69.41	72.29
8	67.2	74.7	93.04	68.23	77.29	82.33	67.57	79.39	81.93

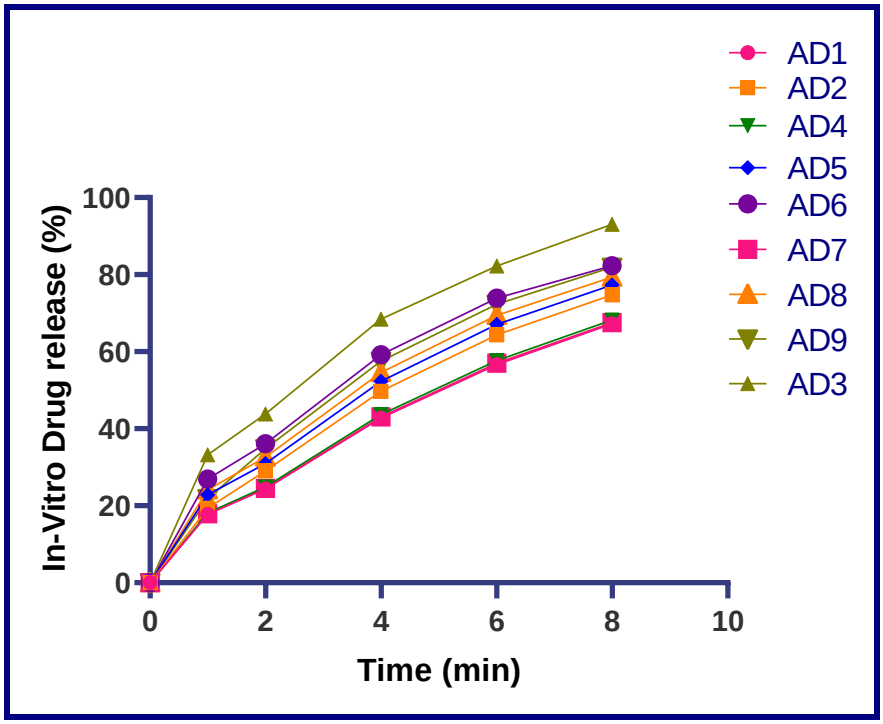

Figure 8: *In vitro* drug release (%) of formulations versus time (min)

DISCUSSION

Figure 1 and 2 represents the interpretation of the FTIR results for both the pure drug and the physical mixture of the drug and excipients. The FTIR spectral analysis of the pure Rimegepant showed characteristic peaks at 3375.78 cm^{-1} (N-H stretch), 3753.76 cm^{-1} (OH bend), 2965. cm^{-1} (C-H bend), 2265.95 cm^{-1} (C=N), and 1725.98 cm^{-1} (C=O). The spectrum of the physical mixture containing Rimegepant and excipients displayed peaks at similar wavenumbers: 3375.78 cm^{-1} (N-H stretch), 3746.05 cm^{-1} (OH bend), 2912.95 cm^{-1} (C-H bend), 2265.95 cm^{-1} (C=N), 1724.98 cm^{-1} (C=O), and an additional peak at 1610.27 cm^{-1} (C=C aromatic).

The comparison of the FTIR spectra of the pure drug and the physical mixture revealed no significant shifts or changes in the characteristic peaks. This suggests that

there are no significant chemical interactions between Rimegepant and the excipients used in the formulation, indicating good compatibility. The additional peak observed at 1610.27 cm^{-1} (C=C aromatic) in the physical mixture spectrum could be attributed to the presence of excipients, and it does not indicate any incompatibility or chemical interactions between the drug and the excipients. In conclusion, the FTIR spectral analysis indicates that Rimegepant is compatible with the excipients used in the formulation, and no significant chemical interactions were observed.

The Differential Scanning Calorimetry (DSC) studies provided further evidence for the compatibility of Rimegepant with the excipients used in the fast dissolving film formulation. The DSC thermogram of pure Rimegepant (Figure 3) showed an endothermic peak at 162.22°C, which corresponds to its melting point. This observation agrees with the previously reported melting point of Rimegepant (166°C). The DSC thermogram of the physical mixture containing both the pure drug and the excipients (Figure 4) exhibited peaks at 137.39°C and 164.45°C. The presence of these peaks suggests that the drug and excipients are present in their individual forms without any significant interaction. This is a crucial observation, as it indicates that the formulation process and the excipients used in the fast dissolving film do not alter the drug's physicochemical properties. In conclusion, the DSC studies support the findings of the FTIR spectral analysis, confirming the compatibility of Rimegepant with the excipients used in the fast dissolving film formulation.

The physicochemical properties of fast dissolving films for various formulations (AD1 to AD9) were evaluated, and the results are presented in Tables 3 and 4. The film thickness ranged from 0.24±0.02 mm to 0.29±0.02 mm, indicating a slight variation in thickness across the formulations. This variation might be attributed to the differences in the composition of each formulation, affecting the overall thickness of the films. However, the thickness of all formulations is within an acceptable range for fast dissolving films. The moisture content varied between 2.6±0.1% and 4.1±0.1%. Higher moisture content can be associated with longer disintegration times and lower mechanical strength. It is crucial to maintain an optimum moisture level to ensure good film properties and quick disintegration. The pH of the formulations ranged from 5.5±0.4 to 6.5±0.6. This range is considered suitable for oral administration, as it is close to the saliva's pH, which is typically around 6.8. Films with a pH close to saliva are less likely to cause irritation and discomfort when placed in the oral cavity. The drug content uniformity varied between 83.2±1.3% and 99.6±1.1%. It is essential to maintain uniform drug content to ensure consistent and predictable drug release. Most formulations exhibited good drug content uniformity, indicating that the manufacturing process was effective in distributing the drug uniformly within the films.

The disintegration time for the formulations ranged from 6.9±0.4 seconds to 11.2±0.7 seconds. A shorter disintegration time is desirable for fast-dissolving films, as it ensures rapid drug release and faster onset of action. Formulation AD5 showed the shortest disintegration time (6.9±0.4 seconds), while AD9 had the longest (11.2±0.7 seconds). The differences in disintegration times could be attributed to variations in the composition and moisture content of each formulation. Tensile strength values ranged from 5.3±0.4 g/cm² to 9.5±0.8 g/cm². Higher tensile strength indicates better mechanical strength and resistance to breakage. Formulation AD8 exhibited the highest tensile strength (9.5±0.8 g/cm²), while AD1 had the lowest (5.3±0.4 g/cm²). The differences in tensile strength could be due to variations in the polymer and plasticizer concentrations in each formulation. Folding endurance values varied between 155±5 and 215±10, representing the film's ability to withstand repeated folding without breaking. Higher folding endurance values indicate better film flexibility. Formulation AD7 demonstrated the highest folding endurance (215±10), and AD1 had the lowest (155±5). The differences in folding endurance might be a result of different ratios of polymer and plasticizer in the formulations, which affect the overall flexibility of the films. In summary, the physicochemical properties of the fast-dissolving films varied across the different formulations. These variations could be attributed to the differences in the composition of each formulation, such as polymer and plasticizer concentrations. The results indicate that it is possible to tailor the properties of fast dissolving films by altering their compositions to achieve desired attributes, such as quick disintegration, high tensile strength, and good folding endurance.

Table 5 presents the results of the analysis of variance (ANOVA) for the quadratic model of disintegration time (R1) concerning the concentrations of HPMC E100 (A) and honey (B). The model was found to be significant, with a p-value of 0.0129. The individual factors, A-HPMC E100 and B-Honey, were also significant, with p-values of 0.0028 and 0.0482, respectively. The interaction term (AB) and the squared terms (A^2 and B^2) were significant as well, with p-values of 0.0324, 0.0437, and 0.0028, respectively. These results indicate that both HPMC E100 and honey concentrations, as well as their interaction, significantly affect the disintegration time of the fast-dissolving films.[14]

The high R^2 value (0.9752) indicates that the model explains 97.52% of the variability in the disintegration time. The adjusted R^2 (0.9339) and predicted R^2 (0.7162) also show a good fit of the model to the data. The adequate precision ratio of 15.2621, which is greater than 4, demonstrates that the model has adequate signal to noise ratio and can be used for predicting disintegration time. The low coefficient of variation (C.V. %) of 3.7865% suggests that the variation in the data is relatively small, and the model is reliable for predicting the disintegration time of fast dissolving films.

Figure 5 presents the contour plot and 3D surface plot of disintegration time (R1) as

a function of two independent variables: the concentration of HPMC E100 (A) and the concentration of honey (B). The contour plot provides a 2D representation of the response, while the 3D surface plot displays the response as a 3D surface. Both plots help visualize the effect of the independent variables on the disintegration time. From the contour plot, we can observe that the contours are elliptical in shape, which indicates an interaction between the two independent variables, HPMC E100 and honey. The elliptical contours show that the effect of one variable on the disintegration time is dependent on the level of the other variable. The 3D surface plot provides a better visualization of the relationship between the independent variables and the response. It can be observed that as the concentration of HPMC E100 (A) and honey (B) increase, the disintegration time generally decreases. This indicates that the combination of higher levels of HPMC E100 and honey results in faster disintegration of the fast-dissolving films.

The ANOVA results for the quadratic model of tensile strength (R2) in relation to HPMC E100 (A) and honey (B) concentrations are shown in Table 7. The model was found to be significant, as indicated by the F-value (12.09) and the p-value (0.0334), which is less than the generally accepted significance level of 0.05. This indicates that the model can be used to predict the tensile strength of the fast-dissolving films based on the concentrations of HPMC E100 and honey. The individual effects of HPMC E100 (A) and honey (B) concentrations, as well as their interaction (AB), were evaluated. The p-value for the HPMC E100 concentration (A) was found to be 0.0248, indicating a significant effect on the tensile strength of the films. Similarly, the p-value for the honey concentration (B) was 0.0049, suggesting a significant influence on tensile strength. The interaction term (AB) has a p-value of 0.0133, indicating a significant interaction between HPMC E100 and honey concentrations in affecting the tensile strength of the fast-dissolving films. This means that the effect of one variable on tensile strength is dependent on the level of the other variable. The quadratic terms for both HPMC E100 (A^2) and honey (B^2) also have significant p-values (0.0431 and 0.0485, respectively), suggesting that the relationship between the independent variables and tensile strength is not linear but quadratic in nature. In conclusion, the ANOVA results for the quadratic model of Tensile Strength (R2) demonstrate that both HPMC E100 and honey concentrations significantly affect the tensile strength of the fast dissolving films, and their interaction is also significant. The model provides a useful tool for optimizing the formulation of the films to achieve the desired tensile strength for better film integrity and handling.[6]

Table 7 presents the fit statistics for the tensile strength (R2) model. The goodness of fit of the model is evaluated using various statistical measures. The standard deviation (Std. Dev.) of the model is 0.5232, which is a measure of the dispersion or spread of the data around the mean. A smaller standard deviation indicates that the data points are close to

the mean, suggesting a better fit of the model.

The R^2 value for the model is 0.9527, indicating that 95.27% of the variability in the tensile strength can be explained by the model. This suggests that the model provides a good fit for the data. The Adjusted R^2 value is 0.8739, which considers the number of independent variables in the model and adjusts the R^2 value accordingly. This value also indicates a good fit of the model to the data. The coefficient of variation (C.V. %) is 7.11%, which is a measure of the relative variability of the data. A lower C.V. % indicates better precision in the model. The Predicted R^2 value is 0.4429, which estimates how well the model can predict future observations. Although this value is lower than the R^2 value, it is still indicative of the model's predictive ability. Lastly, the Adequate Precision value is 9.6372, which measures the signal-to-noise ratio. A ratio greater than 4 is desirable, indicating an adequate model for navigating the design space. In this case, the value of 9.6372 suggests that the model is adequate for predicting tensile strength.

The contour plot and 3D surface plot of tensile strength (R2) shown in Figure 6 provide a graphical representation of the relationship between the concentrations of HPMC E100 (A) and honey (B) and the tensile strength of the fast-dissolving films. These plots help visualize the effect of the two factors and their interactions on the tensile strength of the films. In the contour plot, the lines represent different levels of tensile strength, and the distance between these lines indicates the rate at which tensile strength changes when varying the concentrations of HPMC E100 and honey. When the contour lines are close together, this suggests that the tensile strength changes rapidly with changes in the concentrations of the components. Conversely, when the contour lines are farther apart, the tensile strength changes more gradually. The 3D surface plot provides another way to visualize the relationship between the two factors and the response variable. It shows the tensile strength as a surface over the concentrations of HPMC E100 and honey. The plot's shape can provide insights into the nature of the interactions between the factors and the response. Peaks or valleys in the surface plot indicate regions of high or low tensile strength, respectively.

The ANOVA results for the quadratic model of folding endurance (R3) in relation to HPMC E100 (A) and honey (B) concentrations indicate a significant relationship between the folding endurance of the fast dissolving films and the concentrations of the two factors. The model's F-value of 9.45 and p-value of 0.0469 confirm the model's significance, suggesting that the model can adequately explain the observed variations in folding endurance. The individual factors and their interactions show varying degrees of significance. Honey (B) has a strong influence on folding endurance, with a high F-value of 38.16 and a low p-value of 0.0085. This suggests that honey plays a crucial role in determining the folding endurance of the fast dissolving films. In contrast, HPMC E100 (A) has a lower F-value of 0.1321 and a p-value of 0.0304,

indicating a weaker impact on folding endurance compared to honey. The interaction term (AB) has an F-value of 6.8 and a p-value of 0.0499, indicating a significant interaction between HPMC E100 and honey on folding endurance. This suggests that the combined effect of HPMC E100 and honey concentrations has a notable impact on the folding endurance of the fast dissolving films. The quadratic terms A^2 and B^2 show different levels of significance. A^2 has a very low F-value (0.0009) and a high p-value (0.978), indicating that the quadratic effect of HPMC E100 concentration is not significant in the model. On the other hand, B^2 has an F-value of 2.16 and a p-value of 0.0482, suggesting that the quadratic effect of honey concentration has some significance in determining folding endurance. In conclusion, the ANOVA results for the quadratic model of Folding Endurance (R3) highlight the importance of honey concentration and the interaction between HPMC E100 and honey concentrations in determining the folding endurance of fast-dissolving films. These findings can be utilized to optimize the formulation to achieve the desired folding endurance properties.

The predicted R^2 value of 0.2742 indicates how well the model can predict new data points. Although this value is lower than the R^2 and adjusted R^2 values, it still provides some predictive capability. The adequate precision value of 9.3704 is a measure of the signal-to-noise ratio. A value greater than 4 suggests that the model has adequate precision to predict the response. In summary, the fit statistics for Folding Endurance (R3) indicate that the model is a good fit for the data and has some predictive capability. Optimizing the factors (HPMC E100 and honey concentrations) can help to achieve the desired folding endurance for fast-dissolving films.

The contour plot and 3D surface plot of folding endurance (R3) (Figure 7) are essential tools for visualizing the relationship between HPMC E100 (A) and honey (B) concentrations and the folding endurance of the fast dissolving films. These plots help to understand how the folding endurance is influenced by the two factors, allowing for the optimization of the formulation. The contour plot represents the folding endurance as a function of HPMC E100 and honey concentrations, where each contour line corresponds to a constant folding endurance value. The contour lines' spacing and shape indicate how the folding endurance changes with varying concentrations of the two factors. The 3D surface plot provides a three-dimensional representation of the folding endurance as a function of HPMC E100 and honey concentrations. This plot enables a better understanding of the interactions between the two factors and their combined effect on folding endurance. By analyzing the contour plot and 3D surface plot of Folding Endurance (R3), the optimal concentrations of HPMC E100 and honey can be determined to achieve the desired folding endurance for the fast-dissolving films. This information can guide the development of a robust and efficient formulation with adequate mechanical properties.

The *in vitro* drug release study for all the batches (AD1-AD9) showed in Figure 8 which provides valuable insights into the release profiles of Rimegepant from the fast dissolving films. The study was conducted at different time intervals (0, 1, 2, 3, 4, and 6 minutes). The results demonstrate that the percentage of drug released increased with time for all the batches. Batch AD1 showed a moderate drug release, with 64.7% release at 6 minutes. In contrast, batch AD9 displayed the highest drug release, reaching 90.8% at 6 minutes. This suggests that the formulation of AD9 was more effective in releasing the drug compared to AD1.As we move from AD1 to AD9, the drug release generally shows an increasing trend. This increase in drug release could be attributed to the varying concentrations of the excipients, HPMC E100 and honey, used in each formulation. The excipients could influence the film's properties, such as its disintegration time, tensile strength, and folding endurance, ultimately affecting the rate of drug release. From the results, it can be inferred that optimizing the formulation by adjusting the excipients' concentrations is crucial for achieving the desired drug release profile. The optimal formulation should ensure a rapid release of the drug to provide a fast onset of action, which is a key characteristic of fast dissolving films.

CONCLUSION

In conclusion, this study demonstrates the successful development and characterization of fast dissolving films containing Rimegepant as the active pharmaceutical ingredient. The solvent casting method proved to be an effective technique for formulating the films, with the optimized composition showing desirable physicochemical properties, including appropriate film thickness, moisture content, pH, drug content uniformity, disintegration time, tensile strength, and folding endurance. Moreover, the *in vitro* drug release studies revealed a rapid and effective release of Rimegepant from the formulated films, indicating their potential for enhanced patient compliance and improved therapeutic outcomes. The drug-excipient compatibility studies, including FTIR and DSC analysis, confirmed that there were no significant interactions between Rimegepant and the excipients used in the formulation. This is an essential aspect for ensuring the stability, safety, and efficacy of the final product. The results obtained from this research suggest that Rimegepant loaded fast dissolving films could serve as a promising alternative to conventional oral dosage forms, particularly for patients with difficulties in swallowing or those requiring rapid onset of action. However, further studies on the stability, pharmacokinetics, and clinical efficacy of these films are warranted to fully establish their potential for clinical application.

REFERENCE

1. Lipton RB, Diamond S, Reed M, Diamond ML, Stewart WF. Migraine diagnosis and treatment: Results from the American migraine study II. Headache. 2001; 41(7):638–45.
2. Friedman DI, De Ver Dye T. Migraine and the environment. Headache. 2009 Jun; 49(6):941–52.

3. De Vries T, Al-Hassany L, Maassenvandenbrink A. Evaluating Rimegepant for the treatment of migraine. Taylor and Francis. 2021; 22(8):973–9.
4. Devhare LD, Ghugare AP, Hatwar BP. Method development for determination of water content from various materials by spectrophotometry and it's validation. International Journal of Drug Delivery, 2015, 7(4), 233-240.
5. Devhare LD, Kore PK. A recent review on bioavailability and solubility enhancement of poorly soluble drugs by physical and chemical modifications. Research Chronicle in Health Sciences. 2016, 2(5), 299-308.
6. Scott LJ. Rimegepant: First approval. Drugs. 2020 May 1; 80(7):741–6.
7. Koteswari P, Sravanthi GP, Mounika M, Mohammed Rafi S, Nirosha K. Formulation development and evaluation of Zolmitriptan oral soluble films using 2^2 factorial designs . Int J Pharm Investig. 2016; 6(4):201.
8. Bala R, Sharma S. Formulation optimization and evaluation of fast dissolving film of Aprepitant by using design of experiment. Bulletin of Faculty of Pharmacy, Cairo University. 2018 Dec 1; 56(2):159–68.
9. Londhe VY, Umalkar KB. Formulation development and evaluation of fast dissolving film of Telmisartan. Indian J Pharm Sci. 2012 Mar; 74(2):122.
10. Abdelbary A, Bendas ER, Ramadan AA, Mostafa DA. Pharmaceutical and pharmacokinetic evaluation of a novel fast dissolving film formulation of Flupentixol dihydrochloride. AAPS PharmSciTech. 2014 Dec; 15:1603-10.
11. Upreti K, Kumar L, Anand P, Chawla V. Formulation and evaluation of mouth dissolving films of Paracetamol. 2017 Jan 22; 8(02).
12. Rao NGR, Kistayya C, Kumar G. Design and development of fast dissolving thin films of Losartan potassium. International Journal of Pharmaceutical Sciences and Drug Research. 2016 Jan 25; 8(01).
13. Kurmi R, Ganju K, Lodhi DS, Chouksey K. Formulation, development and evaluation of fast dissolving oral film of anti-migraine drug. World Journal of Pharmaceutical and Medical Research.Vol. 8, 2015.
14. Mashru RC, Sutariya VB, Sankalia MG, Parikh PP. Development and evaluation of fast dissolving film of Salbutamol sulphate. Drug Development and Industrial Pharmacy. 2005 Jan 1; 31(1):25-34.
15. Makhani AA and Devhare LD. Development and validation of vierordt's spectrophotometric method for simultaneous estimation of Drotaverine and Nimesulide combination. Research Chronicle in Health Sciences. 2017, 3(2), 22-28.
16. Makhani AA and Devhare LD. Development and validation of analytical methods for Drotaverine and Nimesulide combination. Research Chronicle in Health Sciences. 2017, 3(3), 40-44.
17. Bansal S, Bansal M, Garg G. Formulation and evaluation of fast dissolving film of an antihypertensive drug. International Journal of Pharmaceutical, Chemical and Biological Sciences. 2013 Oct 1; 3(4).
18. Londhe V, Shirsat R. Formulation and characterization of fast dissolving sublingual film of Iloperidone using box-behnken design for enhancement of oral bioavailability. AAPS PharmSciTech. 2018 Apr 1; 19(3):1392–400.

19. Alkahtani ME, Aodah AH, Abu Asab OA, Basit AW, Orlu M, Tawfik EA. Fabrication and characterization of fast dissolving films containing Escitalopram/Quetiapine for the treatment of major depressive disorder. Pharmaceutics. 2021 Jun 1; 13(6).
20. Ghugare AP, Devhare LD, Hatwar BP. Development and validation of analytical methods for the simultaneous estimation of Nimorazole and Ofloxacin in tablet dosage form. International Journal of Drug Delivery. 2016, 8(3), 96-98.
21. Devhare LD and Gokhale N. Antioxidant and antiulcer property of different solvent extracts of *Cassia tora* linn. Research Journal of Pharmacy and Technology. 2022, 15(3), 1109-1113.
22. Raykar M, Velraj M. Design, development and evaluation of mouth dissolving tablets of Tofacitinib citrate. International Journal of Applied Pharmaceutics. 2022 Jan 1; 14(1):238–45.
23. Hussain MW, Kushwaha P, Rahman MA, Akhtar J. Development and evaluation of fast dissolving film for oro-buccal drug delivery of Chlorpromazine. Indian Journal of Pharmaceutical Education and Research. 2017 Oct 1; 51(4):S539–47.
24. Devhare LD and Gokhale N. In silico anti-ulcerative activity evaluation of some bioactive compound from *Cassia tora* and *Butea monosperma* through moleculer docking approach. International Journal of Pharmaceutical Sciences and Research. 2023, 14(2), 1000-08.
25. Devhare LD and Gokhale N. A brief review on: phytochemical and antiulcer properties of plants (fabaceae family) used by tribal people of Gadchiroli, Maharashtra. International Journal of Pharmaceutical Sciences and Research. 2023, 14(4), 1572-1593
26. Malviya V, Pande S. Development and evaluation of fast dissolving film of Fluoxetine hydrochloride. Research Journal of Pharmacy and Technology. 2021; 14(10):5345-50.
27. Bodhankar SS, Devhare LD, et al. Formulation and *in vitro* evaluation of dental gel containing ethanglic extract of *Mimosa pudica*. European Chemical Bulletin. 2023, 12(Spe. Issue 5), 1293-1299
28. Devhare LD, Bodhankar SS, et al. Important role of food and nutritional security during Covid-19: A survey. European Chemical Bulletin. 2023, 12(Special Issue 5), 1363-1374
29. Tonde TU, Kasliwal RH, Devhare LD. Quantitative estimation of bacoside A in polyherbal memory enhancer syrup for memory boosting activity using HPTLC method. Research Chronicle in Health Sciences. 2016, 2(6), 315-320